IEEE Photonics Journal
An IEEE Photonics Society Publication

Open Access

Metallic Grating on a D-Shaped Fiber for Refractive Index Sensing

Volume 5, Number 5, October 2013

Hai-Tao Yan
Qi Liu
Yang Ming
Wei Luo
Ye Chen
Yan-qing Lu, Senior Member, IEEE

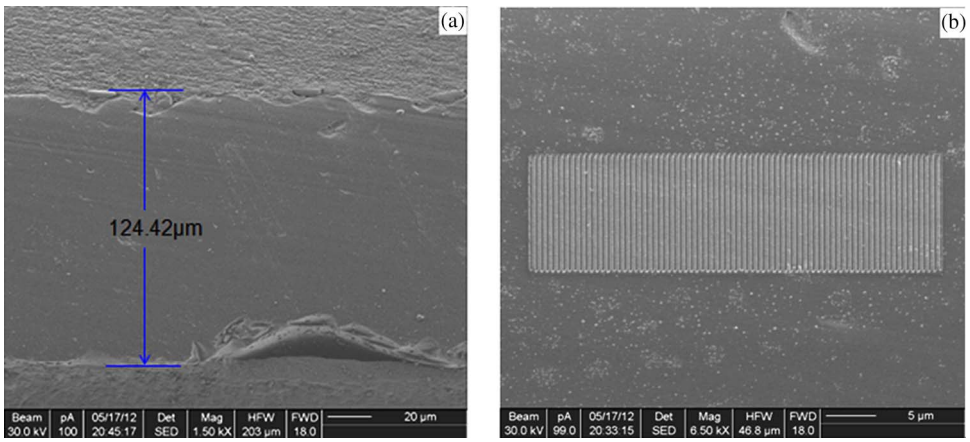

DOI: 10.1109/JPHOT.2013.2284244
1943-0655 © 2013 IEEE

IEEE photonics SOCIETY

IEEE

Metallic Grating on a D-Shaped Fiber for Refractive Index Sensing

Hai-Tao Yan,[1,2] **Qi Liu,**[1] **Yang Ming,**[1] **Wei Luo,**[1] **Ye Chen,**[1] **and Yan-qing Lu,**[1] ***Senior Member, IEEE***

[1]National Laboratory of Solid State Microstructures and College of Engineering and Applied Sciences, Nanjing University, Nanjing 210093, China
[2]College of Physics and Engineering and Key Laboratory of Photoelectric Functional Materials, Henan University of Science and Technology, Luoyang 471003, China

DOI: 10.1109/JPHOT.2013.2284244
1943-0655 ©2013 IEEE

Manuscript received August 19, 2013; revised September 21, 2013; accepted September 23, 2013. Date of current version October 7, 2013. This work was supported in part by the National 973 Program under Contract 2010CB327800, by the National Science Fund for Distinguished Young Scholars under Contract 61225026, and by PAPD and the Fundamental Research Funds for the Central Universities. Corresponding author: Y. Lu (e-mail: yqlu@nju.edu.cn).

Abstract: Metallic grating (MG) with high accuracy is fabricated on the side surface of a D-shaped fiber by using focused ion beam (FIB) machining. The D-shaped fiber is obtained through polishing the cladding of a single-mode fiber away from one side. Then, a thin-film layer of gold is deposited on the flat side surface. A 38-μm-long grating with the pitch of 485 nm is further milled on the gold film. The guiding mode and the surface plasmon polariton mode are thus coupled in the MG through the evanescent field for sensing applications. The refractive indexes of pure water and isopropanol are measured. A sensitivity of 917 nm/RIU is obtained.

Index Terms: Metallic grating (MG), D-shaped fiber, sensor.

1. Introduction

Introducing microstructures on to optical fibers provides them a wide variety of new features, which result in many useful applications in various situations. Tapering or polishing a fiber is one of the important ways to modify the original fiber's structures toward some unusual functions. These attempts include the plastic-clad silica fibers with partly removed cladding [1], side-polished fibers [2]–[4], tapered single-mode fibers [5], tip-polished fibers [6], [7], and D-shaped fibers [8]. Among all of them, the D-shaped fiber presents a unique platform owing to its flat side surface, which is quite convenient in fabricating various surface structures. If a thin metal film is deposited onto the fiber, the surface plasmon polariton (SPP) mode could be excited. Introducing some structures into the film may further enhance its functionality. Very recently, with the emergence of new nanoscale fabrication and characterization techniques, studies on the interaction of electromagnetic radiation with nanostructured metals (e.g., Au and Ag) have become hot research topics, driven by their unique optical properties and promising advantages in optical signal processing and sensing. For example, metallic gratings (MGs) with their periods smaller than the incident wavelength have been widely investigated for various applications, e.g., polarizers [9], biosensors [10], and couplers [11]. In the SPP sensors mentioned above, the excited SPP is normally in the visible band.

In this paper, we fabricate a metallic grating on a D-shaped fiber (MGDF) surface by using focused ion beam (FIB) machining. As this structure could support SPP mode [12]–[16], we have presented a comparative theoretical study on the sensing characteristics of the D-shaped-fiber-based MG.

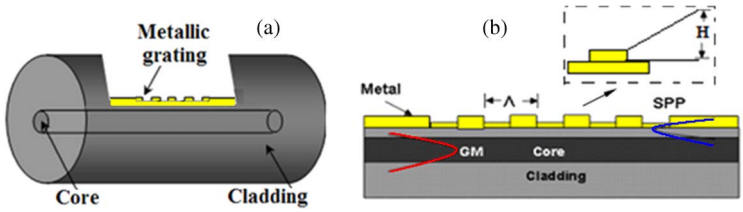

Fig. 1. Schematic diagram of the MG on a D-shaped fiber surface.

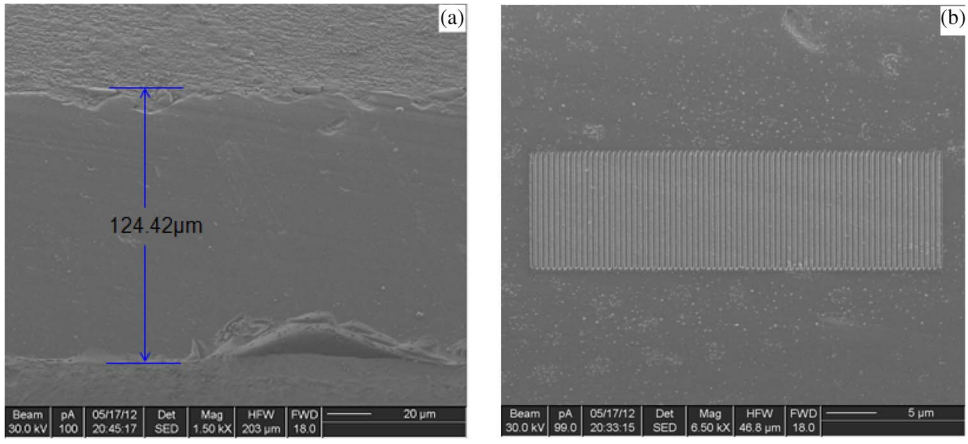

Fig. 2. (a) SEM picture of a D-shaped fiber and (b) the MG (38.8 μm in length) on the polished surface.

The sensing of ambient refractive indexes using the excitation of SPP [12] is measured. The corresponding sensitivity is characterized as the wavelength shift of the reflection spectrum versus the environmental refractive index, which is around the level of $\sim 10^3$ nm/RIU.

2. Design and Fabrication

A standard single-mode silica optical fiber (SMF-28, 125 μm in diameter) is selected for our experimental demonstration. The schematic is shown in Fig. 1, where GM represents the guiding mode of a fiber, H is the height of the grating, and Λ is the period of the grating. The coating of the fiber is removed for further polishing. Then, the fiber is connected to a light source and an optical power meter during side polishing so that we may monitor the process and determine the degree of polishing. Finally, a D-shaped fiber is obtained with its polished surface 2–10 μm away from the core. The distance can be calculated from the width of the surface, as shown in Fig. 2(a). At this time, the transmission loss is about 15–20 dB, which is mainly due to the mode mismatch and surface scattering. Then, the fiber is coated with a 20-nm-thick gold layer on the polished surface by magnetron sputtering. We choose gold due to its relatively low absorption in the infrared and inertness to oxidation when exposed in air.

Fig. 2(a) shows the polished surface of the D-shaped fiber, which is ~ 6 μm away from the core. An MG is then fabricated through FIB milling. In our work, the coupling between the forward core-mode and the backward cladding-mode is considered. Thus, Δn_{eff} $(= n_{\text{c}} + n_{\text{cl}})$ is estimated to be 2.8–3, where n_c and n_{cl} are the effective indexes of the core mode and the cladding mode. According to the phase matching condition, if the exciting SPP wavelength λ_{R} is at 1550-nm telecommunication band, the designed grating period $\Lambda(\sim \lambda_{\text{R}}/\Delta n_{\text{eff}})$ should be around 500 nm. The duty cycle also affects the response wavelength, but its effect is much less than that of the period parameter. The milling is completed using a Ga-ion-based FEI-201 FIB system in a one-step process. A 30-kV 100-pA cylindrical-symmetric beam with a diameter less than 20 nm is utilized in

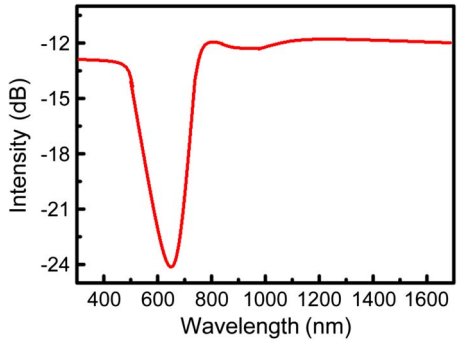

Fig. 3. The transmission spectrum of a D-shaped fiber with Au-coating on its flat surface. No grating is fabricated yet.

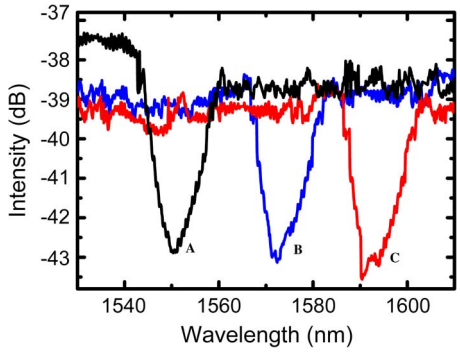

Fig. 4. Measured reflection spectra of an MDGF in (A) pure water, (B) water and isopropanol mixture (1 : 1), and (C) isopropanol, respectively.

order to achieve good milling quality. No other treatment is needed to improve sharpness or accuracy [14]. Fig. 2(b) shows the scanning electron microscopic (SEM) picture of the periodic structures. The MG has period $\Lambda = 485$ nm, and the duty cycle is 50%. The total grating length is only 38.8 μm.

3. Experiments and discussions

Before we characterize the optical properties of MGDF, the transmission spectrum of a D-shaped fiber with a Au film coated on its flat surface is measured. No grating is further fabricated. An Ando AQ6317B optical spectrum analyzer (OSA) and a broadband light source (LDLS-EQ) are used. Fig. 3 shows the result. From the figure, if there is no grating structure, a valley exists at 642 nm in the transmission spectrum, corresponding to a forward SPP excitation. On the other hand, the backward reflection just shows some weak noise in the whole visible-near-infrared band. No evident SPP excitation is found in both directions at the telecom band for such a Au-film-loaded D-shaped fiber.

On the other hand, the optical characterization of the MGDF shown in Fig. 1 is subsequently performed by using an OSA accompanied by an amplified spontaneous emission source (1525–1610 nm). Fig. 4 shows the reflection spectra of the MGDF immersed in pure water, mixture of water and isopropanol (1 : 1), and pure isopropanol, respectively. The wavelength of the valley in the spectrum shifts from 1550.20 to 1571.21 nm and then to 1590.12 nm when the outer environment changes from pure water to pure isopropanol. The spectra have some white noise less than 1 dB. The D-shaped fiber length, the MG length, and the grating amplitude also influence the grating's transmission.

In order to affirm the MG's properties, we analyze the corresponding theory. As is well known, all field components of the modes and the SPP propagating in the D-shaped surface structure along the z-axis contain a common factor $\exp(i\beta^{g,p}z - i\omega t)$, where $\beta^{g,p}$ is the propagation constant, and ω is the radial frequency of radiation connected with the wavelength $\lambda = 2\pi c/\omega$. The superscripts g and p correspond to the guiding mode and the SPP mode, respectively. According to Helmholtz equation, its solution is $u^2/a^2 = \beta^2 - k_0^2 n_i^2$, $r \geq a$; $u^2/a^2 = k_0^2 n_i^2 \beta^2 - \beta^2$, $r \leq a$ in a cylindrical coordinate system, where "a" is the radius of the core, and "u" is the normalized phase constant. If the phase only changes in the Z direction of propagation, the solution can be also used for multilayer structures. The structures we fabricated have five layers, i.e., cladding, core, cladding (buffer), metal, and sensing material; each layer of the structure can be characterized by the following parameters [17]:

$$(\gamma_{\mathrm{i}}^{g,p})^2 = -(k_i^{g,p})^2 = (\beta^{g,p})^2 - k_0^2 n_i^2 \tag{1}$$

where k_0 is the vacuum wavenumber, n_i is the refractive index of the i-layer of the structure, representing cladding, core, cladding (buffer), metal, or sensing material, respectively. As a consequence, a corrugated MG engraved on the surface of the metal layer separated by a buffer from the waveguide layer can be viewed as a reflector, which converts the forward-propagating guiding mode to a backward-propagating SPP (see Fig. 1). The whole process could be viewed as a combination of fiber Bragg reflection and SPP excitation. The amplitude of the grating is H, and its period is Λ. To analyze the grating transmission, we use the exact coupled mode theory, which is also known as a local-normal-mode transfer-matrix method (MTT) [17]–[19]. The period of the grating can be expressed as $\Lambda = \Lambda^{(j+1)} + \Lambda^{(j)}$ [20], [21]. The lengths of the sections with "thick" and "thin" metal layers are equal to $\Lambda k = \pi/2\delta k$, where $\delta k = (\beta_k^g + \beta_k^p)/2$ and $k = (j+1)$, respectively. $\beta_{j+1}^{g,p}$ and $\beta_j^{g,p}$ are the guided-mode (g) and SPP (p) propagation constants in the "thick" $(j+1)$ and the "thin" (j) metal-layer sections (see Fig. 1), respectively. Here, the guided-mode has the core-mode and the cladding mode; the resonance wavelength (λ_{R}) for the core and cladding modes is given by the phase matching condition

$$\frac{2\pi}{\lambda_R}(n_c + n_{cl}) + (k_c - k_{cl}) = \frac{2\pi}{\Lambda} \tag{2}$$

where n_c and n_{cl} are the effective indexes of the core mode and the cladding mode, respectively, and k_{c} and k_{cl} are the coupling coefficients of the core mode and the cladding mode within the core region, respectively. Then, the transmitted power in this structure is given by

$$P = (\delta/a)^2 \sin^2(\alpha l) + \cos^2(\alpha l) \tag{3}$$

where $\delta = 1/2(k_c - k_{cl} + \Delta\beta)$ is the phase mismatch, and $a = \sqrt{|k_{ac}|^2 + \delta^2}$. $\Delta\beta$ is the propagation constant difference between the core mode and the concerned cladding mode, and k_{ac} is the modal coupling coefficient of the core mode and the cladding mode within the core region. We can select the grating period to obtain the resonance wavelength of the structure tune to any desired value. Taking the Durbe model [20], the MG minimum power at the predetermined wavelength at 1550 nm with the $n_{\mathrm{sen}} = 1.33$ is calculated. n_{sen} is the refractive index of sensing material. The refractive index of pure water is 1.33, in Fig. 4, the wavelength of minimum power in the reflection spectrum is at 1550.20 nm, and the experiential results agree well with the calculated results in theory. For the isopropanol mixture and isopropanol measurement, the refractive index of pure isopropanol at 1.5 μm is 1.3739 [21]. The wavelength shifts from 1550.20 to 1571.21 nm (isopropanol mixture) to 1590.12 nm (pure isopropanol). Besides the wavelength shift, the reflected spectra also have some deformation for different liquid index measurements. The major difference is the background reflection. This is because the background reflection is also influenced by the environmental indexes. Furthermore, our spectrum is a combination effect of the SPP and grating. These two parts may have asynchronous spectral response at different operation conditions, which further causes slight spectral deformation.

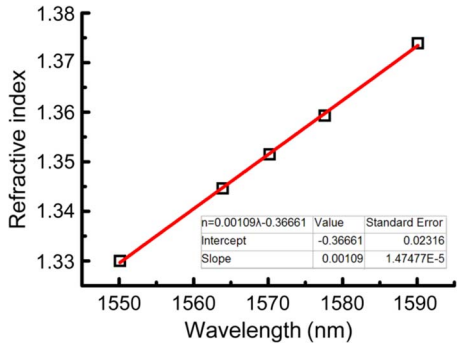

Fig. 5. The valley wavelength as a function of the environmental liquid refractive index. The squares represent the experimental data, whereas the solid line is the linear best-fitting result.

We also measured the pure water and isopropanol mixture 2 : 1 and 1 : 2; the transmission minimum wavelengths are 1563.9 and 1577.6 nm, respectively. Fig. 5 displays the measured resonant wavelength shifts of the valleys and the corresponding best-fitting curve for this MGDF. It shows that the MGDF liquid refractive index sensor has good linearity. This feature is different from the nonlinear index dependence of many normal fiber gratings. As we know, the index sensitivity of SPP is linear and much higher than that of a fiber grating. We believe that it is the combined grating/SPP process that results in this unique index response of an MGDF. Among the measured index range in Fig. 5, the SPP part may dominate the spectral shift so that the net shift is linear-like. However, the nonlinear response may emerge for a wider index range, which still needs further investigation. From the definition of sensor sensitivity $S = \Delta(\lambda_{R1} - \lambda_{R2})/\Delta n_{sen}$ [22], the average sensitivity S of our MGDF sensor is obtained at 917 nm/RIU. Because the 3-dB halfwidth of SPP exciting wavelength $\delta\lambda$ is about 10 nm, the minimum refractive index resolution can be calculated from $\delta\lambda/S$; it is $\sim 1.1 \times 10^{-2}$ RIU, which presents a much higher value than that measured by MGs established on the fiber tip [23]. If we compare the results with Au-film-coated D-shaped fibers with SPP excitation in the visible band, the MGDF also shows some advantages: (1) The operation wavelength is at the 1550-nm telecom band; hence, it is compatible with the widely used G.652 single-mode fibers and related low-cost fiber-optic components. (2) If we compare Figs. 3 and 4, the spectral bandwidth of the valley is much shaper for the MGDF, giving rise to finer minimum refractive index resolution, i.e., the detection limit. In addition, the commercial OSAs normally have much higher resolution in the telecom band than that in the visible band. This feature is further desired for our MGDF.

We have also tried other parameters of the proposed MGDF structure. We find that for a grating with a longer period, the measured spectra response exhibits a redshift, whereas a shorter period results in a blueshift; the height of the grating affects peak intensity of the response as well. In addition, the spectral responses at different temperatures are also investigated. For example, for pure water, the reflection spectra are taken from 20 °C to 60 °C with the increasing step of 10 °C. The corresponding valleys are at 1550.20, 1550.10, 1499.99, 1499.82, and 1499.76 nm, respectively. Thus, the temperature sensitivity of the sensor is around 10–40 pm/°C, which is at the same level as in the previous results [24], [25].

4. Conclusion

In this paper, we have demonstrated an MGDF milled by FIB for refractive index sensing applications. Experimental results of the MG agree well with the calculated results. We select the appropriate period of grating and thickness of the remainder cladding and make the SPP exciting in the communication band. This kind of grating shows high refractive index sensitivity for SPP resonant modes from the metal-dielectric-hybrid cladding structure. In general, our grating utilizes the wavelength sensitivity of Bragg grating and the large evanescent field of D-shaped grating together, it is quite suitable in sensing liquid samples. However, the resonance wavelength mainly depends

on the refraction index. It is hard for our grating to distinguish different liquids with the same refraction index. To further improve the performance of our grating, the absorption spectra of the samples could be measured as well. This is not difficult due to the large evanescent field at the D-shaped surface. In this case, different liquids may be distinguished even if their indexes are the same. This would be an interesting topic to explore in the future.

References

[1] J. K. Kim, D. U. Kim, T. Y. Kim, C. S. Park, B. H. Lee, and K. Oh, "Development of Hard Plastic Clad Fiber (HPCF)-compatible devices and demonstration of HPCF-PON," *IEEE Photon. Technol. Lett.*, vol. 19, no. 11, pp. 834–836, Jun. 2007.

[2] A. Dudu's, R. Blue, and D. Uttamchandani, "Comparative study of microfiber and side-polished optical fiber sensors for refractometry in microfluidics," *IEEE Sensors J.*, vol. 13, no. 5, pp. 1594–1601, May 2013.

[3] S. J. Beecher, R. R. Thomson, B. P. Pal, and A. K. Kar, "Single stage ultrafast laser inscription of a side-polished fiber-like waveguide sensor," *IEEE Sensors J.*, vol. 12, no. 5, pp. 1263–1266, May 2012.

[4] H. T. Sun, E. C. Chang, H. J. Sheng, C. C. Chen, and W. F. Liu, "The tunable dispersion based on side-polished fiber Bragg gratings," *Microw. Opt. Technol. Lett.*, vol. 54, no. 3, pp. 681–684, Mar. 2012.

[5] L. Bilro, N. J. Alberto, L. M. Sa, J. L. Pinot, and R. Nogueira, "Analytical analysis of side-polished plastic optical fiber as curvature and refractive Index sensor," *J. Lightw. Technol.*, vol. 29, no. 6, pp. 864–870, Mar. 2011.

[6] W. Zhang, L. Huang, F. Gao, F. Bo, G. Zhang, and J. Xu, "All-fiber tunable Mach–Zehnder interferometer based on an acousto-optic tunable filter cascaded with a tapered fiber," *Opt. Commun.*, vol. 292, no. 1, pp. 46–48, Apr. 2013.

[7] N. Galina and K. Raman, "Fiber-Bragg-grating-assisted surface plasmon-polariton sensor," *Opt. Lett.*, vol. 31, no. 14, pp. 2218–2220, Jul. 2006.

[8] M. H. Chin, S. F. Wang, and R. S. Chang, "D-type fiber biosensor based on surface-plasmon resonance technology and heterodyne interferometry," *Opt. Lett.*, vol. 30, no. 3, pp. 233–235, Feb. 2005.

[9] S. H. Ahn, J.-S. Kim, and L. J. Guo, "Bilayer metal wire-grid polarizer fabricated by roll-to-roll nanoimprint lithography on flexible plastic substrate," *J. Vac. Sci. Technol. B, Microelectron. Nanom. Struct.*, vol. 25, no. 6, pp. 2388–2391, Nov. 2007.

[10] F. C. Chien, C. Y. Lin, J. N. Yih, K. L. Lee, C. W. Chang, P. K. Wei, C. C. Sun, and S. J. Chen, "Coupled waveguide-surface plasmon resonance biosensor with subwavelength grating," *Biosens. Bioelectron.*, vol. 22, no. 11, pp. 2737–2742, May 2007.

[11] S. Scheerlinck, J. Schrauwen, F. Van Laere, D. Taillaert, D. Van Thourhout, and R. Baets, "Efficient, broadband and compact metal grating couplers for silicon-on-insulator waveguides," *Opt. Exp.*, vol. 15, no. 15, pp. 9625–9630, Jul. 2007.

[12] S. Mani Tripathi, A. Kumar, E. Marin, and J. P. Meunier, "Side-polished optical fiber grating-based refractive index sensors utilizing the pure surface plasmon polariton," *J. Lightw. Technol.*, vol. 26, no. 13, pp. 1980–1985, Jul. 2008.

[13] J. L. Kou, J. Feng, Q. J. Wang, F. Xu, and Y. Q. Lu, "Microfiberprobe-based ultrasmall interferometric sensor," *Opt. Lett.*, vol. 35, no. 13, pp. 2308–2310, Jun. 2010.

[14] G. Brambilla, "Optical fibre nanowires and microwires: A review," *J. Opt.*, vol. 12, no. 4, p. 043001, Mar. 2010.

[15] S. Y. Wu, H. P. Ho, W. C. Law, C. Lin, and S. K. Kong, "Highly sensitive differential phase-sensitive surface plasmon resonance biosensor based on the Mach–Zehnder configuration," *Opt. Lett.*, vol. 29, no. 20, pp. 2378–2380, Oct. 2004.

[16] T. Makino, "Threshold condition of DFB semiconductor lasers by the local-normal-mode transfer-matrix method: Correspondence to the coupled-wave method," *J. Lightw. Technol.*, vol. 12, no. 12, pp. 2092–2099, Dec. 1994.

[17] J. Hong, W. Huang, and T. Makino, "On the transfer matrix method for distributed-feedback waveguide devices," *J. Lightw. Technol.*, vol. 10, no. 12, pp. 1860–1868, Dec. 1992.

[18] N. Matuschek, F. X. Kartner, and U. Keller, "Exact coupled-mode theories for multilayer interference coatings with arbitrary strong index modulations," *IEEE J. Quantum Electron.*, vol. 33, no. 3, pp. 295–302, Mar. 1997.

[19] N. Galina and K. Raman, "Theoretical model of a planar waveguide refractive index sensor assisted by a corrugated long period metal grating," *Opt. Commun.*, vol. 281, no. 12, pp. 1522–1528, Mar. 2008.

[20] D. Marcuse, *Theory of Dielectric Optical Waveguides*, 2nd ed. San Diego, CA, USA: Academic, 1991.

[21] J. Feng, M. Ding, J. L. Kou, F. Xu, and Y. Q. Lu, "An optical fiber tip micro-grating thermometer," *IEEE Photon. J.*, vol. 3, no. 2, pp. 810–814, Oct. 2011.

[22] S. Mani Tripathi, E. Marin, A. Kumar, and J. P. Meunier, "Refractive index sensing characteristics of dual resonance long period gratings in bare and metal-coated D-shaped fibers," *Appl. Opt.*, vol. 48, no. 31, pp. 53–58, Nov. 2009.

[23] J. L. Kou, S. J. Qiu, F. Xu, Y. Q. Lu, Y. Yuan, and G. Zhao, "Miniaturized metal-dielectric-hybrid fiber tip grating for refractive index sensing," *IEEE Photon. Technol. Lett.*, vol. 23, no. 23, pp. 1712–1714, Nov. 2011.

[24] J. L. Kou, M. Ding, J. Feng, Y. Q. Lu, F. Xu, and G. Brambilla, "Microfiber-based Bragg gratings for sensing applications: A review," *Sensors*, vol. 12, no. 7, pp. 8861–8876, Jun. 2012.

[25] J. L. Kou, S. Qiu, F. Xu, and Y. Q. Lu, "Demonstration of a compact temperature sensor based on first-order Bragg grating in a tapered fiber probe," *Opt. Exp.*, vol. 19, no. 19, pp. 18 452–18 457, Sep. 2011.